Anal. Chem. **2000,** *72,* 3965−3971

Accelerated Articles

Coupling High-Pressure MALDI with Ion Mobility/ Orthogonal Time-of-Flight Mass Spectrometry

Kent J. Gillig, Brandon Ruotolo, Earle G. Stone, and David H. Russell*

Laboratory for Biological Mass Spectrometry, Department of Chemistry, Texas A&M University, College Station, Texas 77843

Katrin Fuhrer, Marc Gonin, and Albert J. Schultz

Ionwerks, Inc., 2472 Bolsover, Suite 255, Houston, Texas 77005

A new ion mobility/time-of-flight mass spectrometer employing a high-pressure MALDI source has been designed and tested. The prototype instrument operates at a source/drift cell pressure of 1−10 Torr helium, resulting in a mobility resolution of ~25. A small time-of-flight mass spectrometer (20 cm) with a mass resolution of up to 200 has been attached to the drift cell to identify (in terms of mass-to-charge ratio) the separated ions. A simple tripeptide mixture has been separated in the drift tube and mass identified as singly protonated species. The ability to separate peptide mixtures, e.g., tryptic digest of a protein, is illustrated and compared to results obtained on a high-vacuum time-of-flight instrument.

A major focus of current bioanalytical research involves development of rapid, efficient separation methods that can be interfaced to mass spectrometry.[1,2] Mass spectrometry is attractive for analyzing biomolecules because molecular weight and primary structural information can be obtained from a single experiment. The analytical utility of mass spectrometry for biological applications has expanded with advances in separations−mass spectrometry. For example, major progress has been made in combining separations−mass spectrometry with electrospray ionization (ESI), especially with high-performance liquid chromatography (HPLC)−MS[3−5] and capillary electrophoresis (CE)−MS.[6] Despite the progress made in chromatography−MS, the most popular separations−MS method for proteins is 2-D gel electrophoresis and mass spectral analysis of the "spots" on the gel.[7,8] The utility of gel-MS can be extended further by incorporating proteolytic digestion of the "spot" on the gel, commonly referred to as "in-gel digestion", and mass analysis of the peptides to generate a peptide mass map.[9] Although in-gel digestion/peptide mass mapping can be cumbersome and labor intensive, it has advantages over conventional HPLC−MS or CE−MS. For example, the time scales for HPLC and CE separations are really not compatible with the time scale of MS.[10] As a case in point, HPLC analysis time is quite extensive; separation requires several minutes to hours, whereas the mass spectral data can be acquired at kilohertz (time-of-flight) to hertz (FTMS) rates, depending on the type of mass spectrometer that is used. The time scale for separation limits the sample throughput, and this is an inefficient use of the mass spectrometer. Although CE separations are more rapid than HPLC, minutes are required and the mass spectral data are still acquired at much higher rates.[11]

(1) Beale, S. C. *Anal. Chem*. **1998**, *70*, 279R−300R.
(2) Regnier, F.; Huang G. *J. Chromatogr., A* **1996**, *750*, 3−10 (4th International Symposium on Hyphenated Techniques in Chromatography and Hyphenated Chromatographic Analyzers).
(3) Niessen, W. M. A.; Tinke, A. P. *J. Chromatogr., A* **1995**, *703*, 37−57.
(4) Gelpi, E. *J. Chromatogr., A* **1995**, *703*, 59−80.
(5) Slobodnik, J.; van Baar, B. L. M.; Brinkman, U. A. *J. Chromatogr., A* **1995**, *703*, 81−121.
(6) Cai, J.; Henion, J. *J. Chromatogr., A* **1995**, *703*, 667.
(7) Wilm, M.; Shevchenko, A.; Houthaeve, T.; Breit, S.; Schweigerer, L.; Fotsis, T.; Mann, M. *Nature* **1996**, *379*, 6564, 466−469.
(8) Jungblut, P.; Thiede, B. *Mass Spectrom. Rev.* **1997**, *16*, 145−162.
(9) Pu, L.; Foxworth, W. B.; Kier, A. B.; Annan, R. S.; Carr, S. A.; Edmondson, R. D.; Russell, D. H.; Wood, W. G.; Schroeder, F. *Protein Expression Purif.* **1998**, *13*, 337−348.
(10) Holland, J.; Enke, C. G.; Allison, J.; Stults, J. T.; Pinkston, D.; Newcome, B.; Watson, J. *Anal. Chem*. **1983**, *55*, 997A−1012A.
(11) Banks, J. F., Jr.; Dresch, T. *Anal. Chem*. **1996**, *68*, 1480−1485.
(12) Wu, C.; Siems, W. F.; Asbury, G. R.; Hill, H. H., Jr. *Anal. Chem*. **1998**, *70*, 4929.

10.1021/ac0005619 CCC: $19.00
Published on Web 07/29/2000

Only recently has the potential of ion mobility as a separations method for biological compounds been seriously considered.[12−21] Ion mobility (IM), which separates gas-phase ions on the basis of collision cross sections-to-charge ratios (Ω/z), can be combined with mass spectrometry as a structural probe, viz. to determine conformations of peptide and protein ions as well as dynamics of conformational changes.[22−45] In the majority of this work, electrospray ionization is used to introduce ions into the IM drift tube, but almost all conceivable ion sources have been used with ion mobility, e.g., laser desorption, electron impact, cluster sources, and arc discharge.[46] There may be considerable advantages associated with using MALDI in combination with IM. For example, electrospray ionization of peptides, proteins, and DNA yields a distribution of charge states (m/z values), whereas MALDI yields primarily the singly charged protonated molecule, $[M + H]^+$. Electrospray ionization is performed in a continuous mode; thus, ions must be gated into the drift cell or accumulated in an ion trap[17] and then injected into the drift cell, whereas MALDI is performed in a pulsed mode, and this facilitates collection of the arrival time distribution of the ions. In all but a few instances, ion formation of biological compounds by MALDI is performed under high vacuum. But several groups have shown that it is possible to perform MALDI of biological compounds under high-pressure conditions.[47−50]

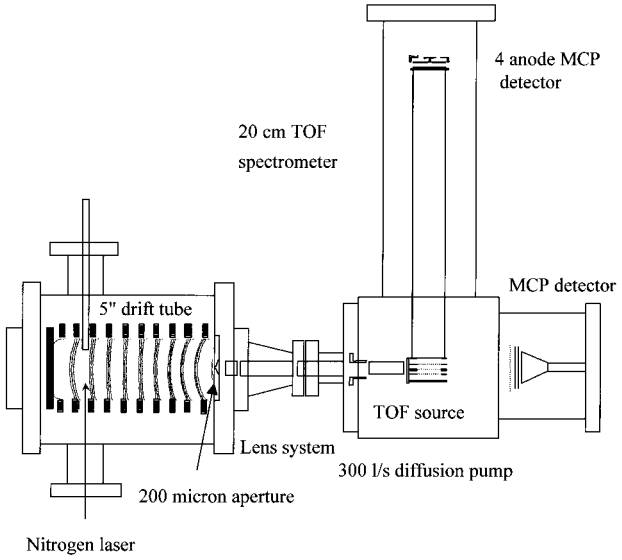

Figure 1. Schematic diagram of the high-pressure MALDI/IM-o-TOF apparatus.

In the experiments described herein, ions are formed directly in the IM drift tube at its operating pressure (1−10 Torr helium) using MALDI. The ion mobility distribution can be recorded independent of the mass spectral data or simultaneously in a mass-resolved IM mode using a time-of-flight (TOF) mass spectrometer positioned perpendicular to the drift cell axis (o-TOF).[17,51] Recently, this combination has proved to be particularly effective for rapid analysis of mobility distributions; however, coupling of a mobility chamber to an orthogonal time-of-flight mass spectrometer was first described in the literature at a much earlier date (1967).[52,53] An instrument designed in this manner provides a straightforward approach for the analysis of proteins, separating and identifying ions by volume/charge and m/z.

EXPERIMENTAL SECTION

The samples, including the thermally denatured "in-solution" tryptic digest of lysozyme, were prepared for MALDI using the

(13) Liu, Y. S.; Valentine, S. J.; Counterman, A. E.; Hoaglund C. S.; Clemmer, D. E. *Anal. Chem*. **1997**, *69*, A728.
(14) Guevremont R.; Siu, K. W. M.; Wang, J. Y.; Ding, L. Y. *Anal. Chem*. **1997**, *69*, 3959.
(15) Wu, C.; Klasmeier, J.; Hill, H. H. *Rapid Commun. Mass Spectrom*. **1999**, *13*, 1138.
(16) Valentine, S. J.; Counterman, A. E.; Hoaglund-Hyzer, C. S.; Clemmer D. E. *J. Phys. Chem. B* **1999**, *103*, 1203.
(17) Henderson, S. C.; Valentine, S. J.; Counterman, A. E.; Clemmer, D. E. *Anal. Chem*. **1999**, *71*, 291.
(18) Valentine, S. J.; Counterman, A. E.; Hoaglund, C. S.; Reilly, J. P.; Clemmer, D. E. *J. Am. Soc. for Mass Spectrom*. **1998**, *9*, 1213.
(19) Hoaglund, C. S.; Valentine, S. J.; Sporleder, C. R.; Reilly, J. P.; Clemmer D. E. *Anal. Chem*. **1998**, *70*, 2236.
(20) Li, J. W.; Taraszka, J. A.; Counterman, A. E.; Clemmer, D. E. *Int. J. Mass Spectrom*. **1999**, *187*, 37.
(21) Counterman, A. E.; Valentine, S. J.; Srebalus, C. A.; Henderson, S. C.; Hoaglund, C. S.; Clemmer, D. E. *J. Am. Soc. for Mass Spectrom*. **1998**, *9*, 743.
(22) Jarrold, M. F. *Acc. Chem. Res*. **1999**, *32*, 360.
(23) Hudgins, R. R.; Jarrold, M. F. *J. Am. Chem. Soc*. **1999**, *121*, 3494.
(24) Mao, Y.; Woenckhaus, J.; Kolafa, J.; Ratner, M. A.; Jarrold, M. F. *J. Am. Chem. Soc*. **1999**, *121*, 2712.
(25) Hudgins, R. R.; Mao, Y.; Ratner, M. A.; Jarrold, M. F. *Biophys. J*. **1999**, *76*, 1591.
(26) Hudgin, R. R.; Woenckhaus, J.; Jarrold, M. F. *Int. J. Mass Spectrom*. **1997**, *165*, 497.
(27) Clemmer, D. E.; Jarrold, M. F. *J. Mass Spectrom*. **1997**, *32*, 577.
(28) Shelimov, K. B.; Jarrold, M. F. *J. Am. Chem. Soc*. **1997**, *13*, 2987.
(29) Mesleh, M. F.; Hunter, J. M.; Shvartsburg, A. A.; Schatz, G. C.; Jarrold, M. F. *J. Phys. Chem. A* **1997**, *101*, 968.
(30) Woenckhaus, J.; Mao, Y.; Jarrold, M. F. *J. Phys. Chem. B* **1997**, *101*, 847.
(31) Shelimov, K. B.; Clemmer, D. E.; Hudgins, R. R.; Jarrold, M. F. *J. Am. Chem. Soc*. **1997**, *119*, 2240.
(32) Mesleh, M. F.; Hunter, J. M.; Shvartsburg, A. A.; Schatz G. C., Jarrold, M. F. *J. Phys. Chem*. **1996**, *100*, 16082.
(33) Valentine, S. J.; Counterman, A. E.; Clemmer, D. E. *J. Am. Soc. Mass Spectrom*. **1997**, *8*, 954.
(34) Valentine, S. J.; Anderson, J. G.; Ellington, A. D.; Clemmer, D. E. *J. Phys. Chem. B* **1997**, *101*, 3891.
(35) Valentine, S. J.; Clemmer, D. E. *J. Am. Chem. Soc*. **1997**, *119*, 3558.
(36) Wyttenbach, T.; von Helden G.; Bowers, M. T. *J. Am. Chem. Soc*. **1996**, *118*, 8355.
(37) von Heldon, G.; Wyttenbach, T.; Bowers, M. T. *Int. J. of Mass Spectrom. Ion Pro*cesses **1995**, *146*, 349.
(38) von Helden, G.; Wyttenbach, T.; Bowers, M. T. *Science* **1995**, *267*, 1483.
(39) Clemmer, D. E.; Hudgins, R. R., Jarrold, M. F. *J. Am. Chem. Soc*. **1995**, *117*, 10141.
(40) Wyttenbach, T.; Batka, J. J., Jr.; Gidden, J.; Bowers, M. T. *Int. J. Mass Spectrom*. **1999**, *193*, 143−152.
(41) Gidden, J.; Wyttenbach, T.; Batka, J. J., Jr.; Weis, T.; Jackson, A. T.; Scrivens, J. H.; Bowers, M. T. *J. Am. Soc. Mass Spectrom*. **1999**, *10*, 883−895.
(42) Gidden, J.; Jackson, A. T.; Scrivens, J. H.; Bowers, M. T. *Int. J. Mass Spectrom*. **1999**, *188*, 121−130.
(43) Wyttenbach, T.; Witt, M.; Bowers, M. T. *Int. J. Mass Spectrom*. **1999**, *182/183*, 243−252.
(44) Wyttenbach, T.; Bowers, M. T. *J. Am. Soc. Mass Spectrom*. **1999**, *10*, 9−14.
(45) Lee, S.; Wyttenbach, T.; Bowers, M. T. *Int. J. Mass Spectrom. Ion Processes* **1997**, *167/168*, 605−614.
(46) Eiceman, G. A. *Ion Mobility Spectrometry*; CRC Press: Boca Raton, 1994.
(47) Gillig, K. J.; Russell, D. H.; Fuhrer, K.; Gonin, M.; Schultz, A. J. *The 47th ASMS Conf. on Mass Spectrom. and Allied Topics*, Dallas, TX, 1999.
(48) Laiko, V. V.; Burlingame, A. L. *The 47th ASMS Conf. on Mass Spectrom. and Allied Topics*, Dallas, TX, 1999; p 49.
(49) Verentchikov, A.; Smirnov, I.; Vestal, M. *The 47th ASMS Conf. on Mass Spectrom. and Allied Topics*, Dallas, TX, 1999; p 39.
(50) Laiko, V. V.; Baldwin, M. A.; Burlingame, A. L. *Anal. Chem*. **2000**, *72*, 652−657.
(51) Russell, D. H.; Gillig, K. J.; Stone, E.; Park, Z.-Y.; Fuhrer, K.; Gonin, M.; Schultz, A. J. *Proc. SPIE* **2000**, *3926*, 69−78.
(52) Mcknight, L. G.; McAffee, K. B.; Sipler, D. P. *Phys. Rev*. **1967**, *164*, 62.
(53) McDaniel, E. W.; Mason, E. A. *The Mobility and Diffusion of Ions in Gases*; Wiley: New York, 1973; pp 68−72.

conventional "dried droplet" method.[54] The peptide/protein samples and MALDI matrixes were purchased from Sigma Chemicals Co. (St. Louis, MO) and dissolved in methanol to obtain matrix/analyte molar ratios of 100−1000/1. Sequencing grade-modified trypsin was purchased from Promega (Madison, WI). Chicken egg white lysozyme was dissolved in aqueous 50 mM ammonium bicarbonate (Sigma) solution to make a 1 μM protein solution and then incubated at 90 °C for 20 min in an airtight microcentrifuge tube. Following incubation, placing the protein in an ice/water bath quenched the denaturation. The thermally denatured protein was digested with trypsin at 37 °C for 4 h using a 40/1 (weight of substrate/weightt of trypsin) concentration. A saturated solution of 2′,4′,6′-trihydroxyacetophenone (Aldrich) in methanol (HPLC grade, Fisher) was added to the protein solution to obtain a mixed protein/matrix solution with a 1000/1 matrix-to-analyte ratio. Picomole amounts of total material were applied directly to an insulated stainless steel probe tip and inserted into the mobility drift cell using a standard vacuum lock assembly.

The vacuum system is divided into two sections, the IM chamber and the o-TOF analyzer, separated by a 200-μm-diameter aperture (see Figure 1). The IM chamber contains the MALDI ion source and mobility drift cell and is operated at 1−10 Torr He (99.99%). The o-TOF analyzer consists of primary beam optics, the extraction region, and the time-of-flight analyzer, maintained at a pressure of 5×10^{-6}−5×10^{-5} Torr by a 300 L/s Edwards Diffstak diffusion pump. An additional microchannel plate detector positioned behind the extraction region is used to measure the arrival time distribution (ATD) of the ions exiting the mobility chamber.

Ions are formed in the drift cell by irradiating the sample deposited on the direct insertion probe with the output from a focused nitrogen laser (337 nm, 20 Hz pulse frequency) at a grazing angle of ∼30° from the drift cell axis. The laser duration is ∼4 ns, and the laser formed plume is quickly cooled by buffer gas collisions reducing the initial spatial spread. There are no detrimental effects of forming ions in the drift cell at low laser powers (threshold, typically used for MALDI). In particular, the effect on the mobility resolution is negligible and defined primarily by the diffusion of ions in the drift cell.

The drift cell consists of 10 0.250-in.-thick, 4.00-in.-outer diameter, 3.00-in.-inner diameter stainless steel rings spaced 0.250 in. apart by $^5/_{16}$-in.-diameter ceramic balls. A linear field is established using a resistor chain of 1-MΩ, high-precision (±1%) and high-voltage (5 kV) resistors. Although the mobility resolution is highest when a linear field is used, the preferred setup is to increase the drift cell sensitivity by focusing the ions using nonlinear fields formed by adjusting the voltages on the drift cell back plate, first ring, and last ring. For example, if the same potential is applied to the back plate and the first ring while the last ring is held at a potential that doubles the field strength between the last ring and the aperture plate, a nonlinear field is obtained throughout the drift cell volume keeping ions confined near the drift cell axis and focused onto the exit aperture. The ion transmission is increased by a factor of 5 over a linear field and the mobility resolution only decreases by a few percent. An example of the preferred configuration including the equipotential lines inside the drift cell is shown in Figure 1.

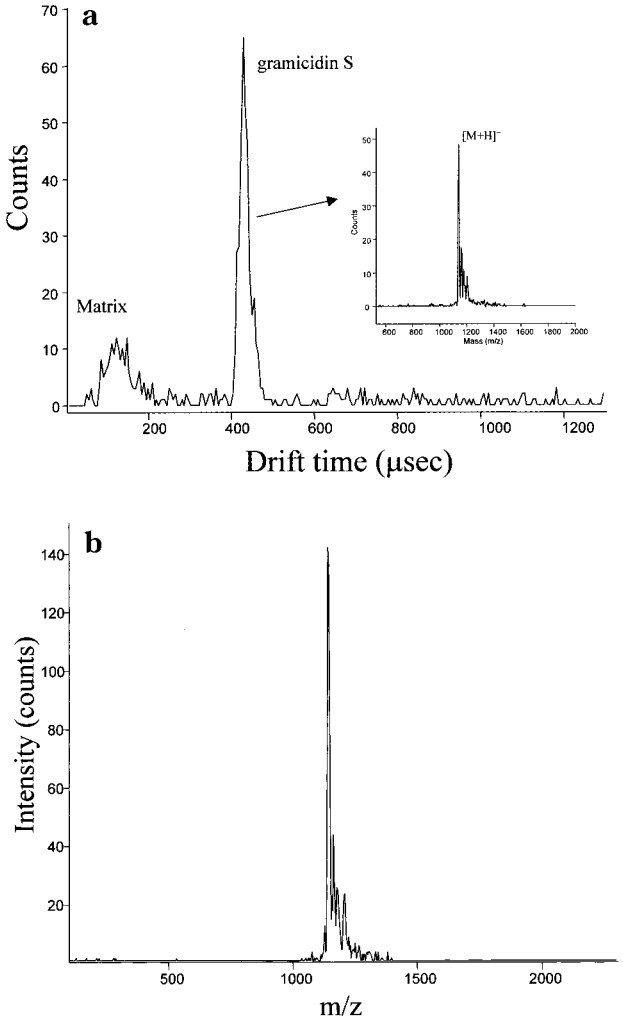

Figure 2. (a) Ion mobility spectrum and mass spectrum (inset) of gramicidin S formed by MALDI demonstrating ion mobility separation and mass identification capability. (b) Mass spectrum acquired using 10 fmol of gramicidin S deposited on the probe tip.

After exiting the 200-μm-diameter aperture, ions are focused into the extraction region of the time-of-flight analyzer by a series of electrodes. The start signal to measure the time-of-flight is coincident with pulsing the extraction region with a high-voltage pulser (Ionwerks, Inc.) The ions are extracted orthogonally and accelerated to 2.5 kV into the 20-cm-long drift tube and detected by a four-anode microchannel plate detector (Ionwerks, Inc.) (see Figure 1).[55] The flight times range from 3 to 60 μs (50−15000 amu), and a mass resolution of 200 is achieved with an extraction field strength of 38 V/mm. In the nonpulsed mode, the ion ATD can be measured with the on-axis microchannel plate detector (Galileo) (see Figure 1). Both detector signals are processed in an ion-counting mode by a time-to-digital converter (Ionwerks model TDCX4). The mass spectra can then be used either for verification of individual mobility peaks or entered into a graphing program, Grams/32, to display three-dimensional representations of m/z versus mobility drift time. Because the mobility drift times are 10−100 times greater than the mass analyzer times, the mass spectra can be signal averaged to increase the S/N ratios. The MALDI time-of-flight mass spectra were acquired on a PerSeptive

(54) Park, Z.-Y.; Russell, D. H., *Anal. Chem.* **2000**, *72*, 2667−2670.
(55) Barbacci, D. C.; Russell, D. H.; Schultz, J. A.; Holocek, J.; Ulrich, S.; Burton, W.; Van Stipdonk, M. *J. Am. Soc. Mass Spectrom.* **1998**, *9*, 1328−1333.

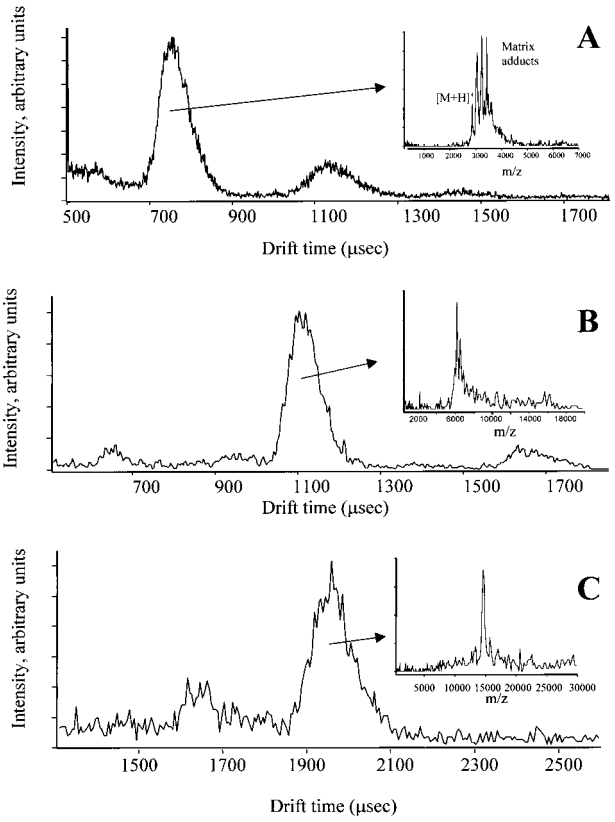

Figure 3. Mobility spectra and corresponding mass identification (inset) of MALDI generated model proteins: (A) melittin, (B) bovine insulin, and (C) chicken egg white lysozyme.

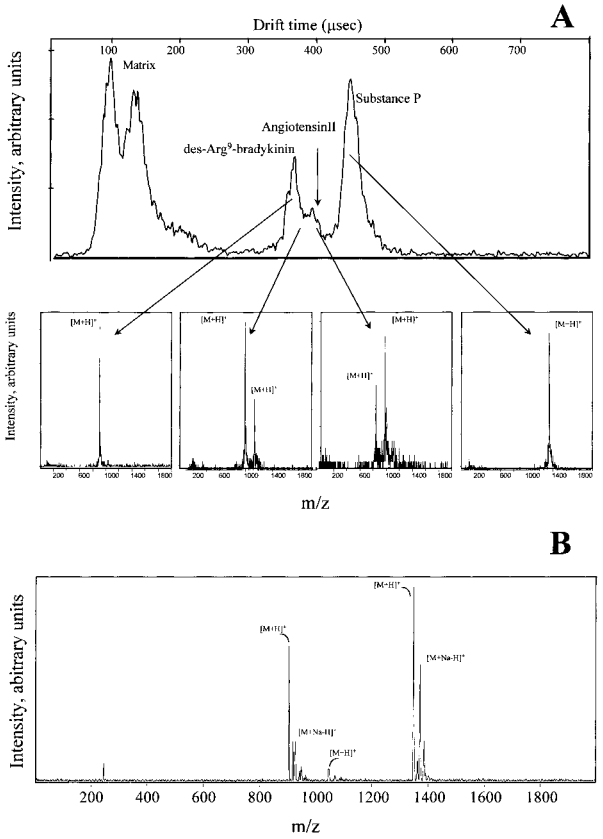

Figure 4. (A) Ion mobility spectrum of a mixture of three peptides (des-Arg-9-bradykinin, angiotensin II, and substance P) formed by MALDI with corresponding mass identification at selected drift times. (B) Mass spectrum of a mixture of three peptides (des-Arg-9-bradykinin, angiotensin II, and substance P) acquired under high-vacuum conditions.

Biosystems Voyager Elite XL TOF reflection mass spectrometer (PerSeptive Biosystems, Inc., Farmingham, MA) as previously described.[56]

RESULTS AND DISCUSSION

The objective for this work is to develop an IM-o-TOF mass spectrometer for rapid analysis of mixtures of peptides, proteins, and other biological samples. That is, we hope to develop a gas-phase analog to SDS−PAGE gel electrophoresis that can be coupled to a mass analyzer. Because IM separates ions on the basis of collision cross sections (collision cross section-to-charge (Ω/z) ratios) and ion−neutral interaction potentials,[53] this information can be combined with more classical mass spectrometry structural data, e.g., fragmentation patterns, ion−molecule reactivity, and H/D exchange chemistry, for structural determination. Our approach utilizes MALDI for ion formation because the analyte is formed with a narrow distribution of charge states, and for most analytes, only singly charged analyte ions are produced. Figure 2a contains an IM spectrum obtained for gramicidin S using 2′,4′,6′-trihydroxyacetophenone as the matrix. The total acquisition time for this mass spectrum was ∼1 s (20 laser shots). We have used other matrixes for gramicidin S and similar peptides, and we do not see significant differences in the data. The spectrum consists of a single peak (at 420 μs drift time) corresponding to protonated gramicidin S, $[M + H]^+$ and the sodium/potassium cationized gramicidin S, $[M + Na]^+/[M + K]^+$ (see inset mass spectrum Figure 2a). The signals at shorter drift times are due to atomic species, primarily Na^+ and K^+. Figure 2b contains a mass spectrum of gramicidin S obtained using α-cyano-4-hydroxycinnamic acid as the matrix. The spectrum was acquired from 10 fmol of deposited peptide with a total acquisition time of ∼2 min.

Figure 3 contains mobility spectra for melittin, (MW 2846.5; α-cyano-4-hydroxycinnamic acid matrix), bovine insulin (MW 5734.7; 2′,4′,6′-trihydroxyacetophenone matrix), and lysozyme (MW 14 307; 2′,4′,6′-trihydroxyacetophenone matrix) with MALDI mass spectra inset in each figure showing the mass range capability of the IM-o-TOF for singly charged species. In each example, the mobility drift cell was operated using a ratio of electric field strength to gas number density (E/N) of ∼30 V/cm·Torr; e.g., 350 V at 1 Torr. Under these conditions, each analyte forms higher molecular weight clusters and/or adducts with the matrix. For example, the inset of Figure 3A shows the mass spectrum obtained by sampling the ions entering the TOF ion source at a drift time of ∼700 μs. A prominent signal is obtained for the $[M + H]^+$ ion, but the dominant ion signal corresponds to matrix adducts, e.g., $[M + (matrix)_n]^+$, where $n = 1-3$. The mobility spectrum for melittin also contains a signal at ∼1150 μs which has a mass that corresponds to the peptide dimer attached to matrix, e.g., $[2M + matrix]^+$, where M represents the intact melittin. The ion mobility spectra and mass spectra for bovine insulin (Figure 3B) and lysozyme (Figure 3C) are very similar to

(56) Edmondson, R. D.; Russell, D. H. In *Mass Spectrometry of Biological Materials*; McEwen, C. N., Larsen, B. S., Eds.; Marcel-Dekker: New York, 1998; Chapter 2.

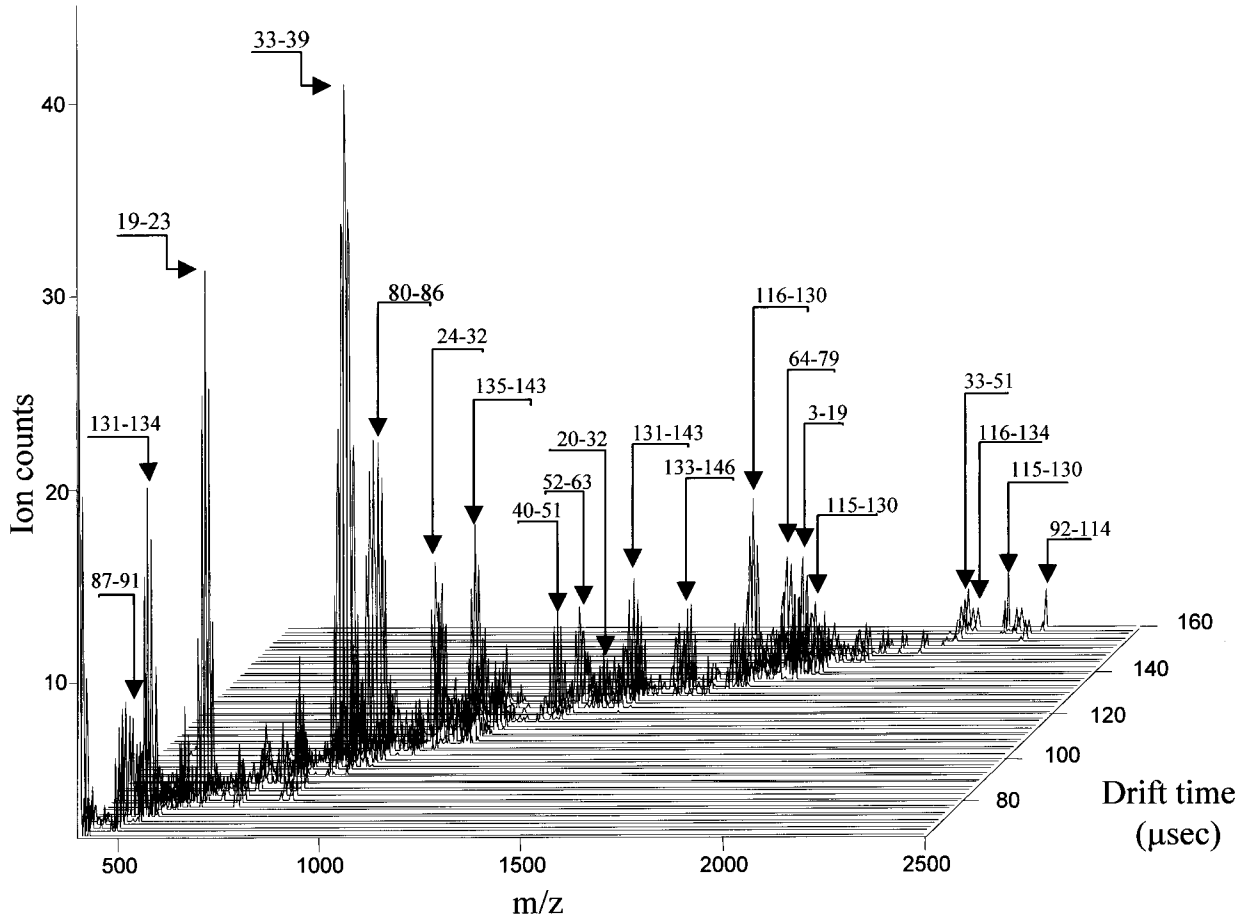

Figure 5. 3D plot of *m*/*z* versus IM drift time of a tryptic digest of thermally denatured chicken egg white lysozyme.

Table 1

Start-End	M+H$^+$(avg.)	Sequence	Start-End	M+H$^+$(avg.)	Sequence
87-91	517.56	TPGSR	131-143	1547.78	NRCKGTDVQAWIR
131-134	520.63	NRCK	133-146	1593.86	CKGTDVQAWIRGCR
19-23	606.75	KVFGR	116-130	1676.89	IVSDGNGMNAWVAWR
33-39	874.93	HGLDNYR	64-79	1754.85	NTDGSTDYGILQINSR
80-86	937.02	WWCNDGR	3-19	1785.34	SLLILVLCFLPLAALGK
24-32	993.23	CELAAAMKR	115-130	1805.06	KIVSDGNGMNAWVAWR
135-143	1046.17	GTDVQAWIR	33-51	2125.37	HGLDNYRGYSLGNWVCAAK
40-51	1269.46	GYSLGNWVCAAK	116-134	2178.50	IVSDGNGMNAWVAWRNRCK
52-63	1429.49	FESNFNTQATNR	32-51	2281.67	RHGLDNYRGYSLGNWVCAAK
20-32	1452.78	VFGRCELAAAMKR	92-114	2338.71	NLCNIPCSALLSSDITASVNCAK

Coverage Map for Ion Mobility Experiment

The matched peptides cover **97% (144/147 AA's)** of the protein.

```
1           11          21          31          41          51          61          71
MRSLLILVLC  FLPLAALGKV  FGRCELAAAM  KRHGLDNYRG  YSLGNWVCAA  KFESNFNTQA  TNRNTDGSTD  YGILQINSRW
81          91          101         111         121         131         141
WCNDGRTPGS  RNLCNIPCSA  LLSSDITASV  NCAKKIVSDG  NGMNAWVAWR  NRCKGTDVQA  WIRGCRL
```

that for melittin. The analyte + matrix adducts for bovine insulin are resolved in the mass spectrum; however, the mass resolution is not sufficient to resolve adduct ions in the mass spectrum of lysozyme. The peak centroid for the lysozyme ion appears at *m*/*z* 14 662 (average MW 14 307) suggesting that the signal corresponds to $[M + (matrix)_n]^+$, where the average value for *n* is 2. Hill et al. also observed cluster formation of analyte with solvent in electrospray ionization IM experiments, and they showed that solvation can be reduced by heating the drift gas.[57] We have not yet performed experiments on the effect of drift gas temperature on MALDI ion formation, but we anticipate that matrix adduction can be reduced by raising the cell temperature.

(57) Yong, H. C.; Hill, H. H.; Wittmer, D. P. *Int. J. Mass Spectrom. Ion Processes* **1996**, *154*, 1−13.

Table 2.

Start-End	M+H$^+$(avg.)	Sequence	Start-End	M+H$^+$(avg.)	Sequence
87-91	517.56	TPGSR	52-63	1429.49	FESNFNTQATNR
19-23	606.75	KVFGR	20-32	1452.78	VFGRCELAAAMKR
33-39	874.93	HGLDNYR	116-130	1676.89	IVSDGNGMNAWVAWR
80-86	937.02	WWCNDGR	64-79	1754.85	NTDGSTDYGILQINSR
135-143	1046.17	GTDVQAWIR	115-130	1805.06	KIVSDGNGMNAWVAWR

Coverage Map for High Vacuum MALDI

The matched peptides cover **57% (85/147 AA's)** of the protein.

```
1          11         21         31         41         51         61         71
MRSLLILVLC FLPLAALGKV FGRCELAAAM KRHGLDNYRG YSLGNWVCAA KFESNFNTQA TNRNTDGSTD YGILQINSRW
81         91         101        111        121        131        141
WCNDGRTPGS RNLCNIPCSA LLSSDITASV NCAKKIVSDG NGMNAWVAWR NRCKGTDVQA WRGCRL
```

Figure 4 contains an ion mobility spectrum for a mixture of three peptides codeposited onto the probe tip in equal amounts (~1 pmol) and mixed with α-cyano-4-hydroxycinnamic acid as the matrix. The ion signals at short drift times correspond to Na^+, K^+, and matrix ions, and these signals show a strong dependence on laser power similar to MALDI performed under vacuum. At longer drift times, signals due to the three peptides eluting the drift cell are detected. The inset mass spectra are identified as indicated by the arrows with their origins positioned at the mass spectrometer sampling time. Although mobility resolution is not sufficient to completely separate signals for des-Arg^9-bradykinin (MW 904) and angiotensin II (MW 1046), the two corresponding mass spectral peaks provide verification of the assignments. A plot of $[M + H]^+$ ion abundances versus drift time for the two peptides provides accurate information for relative Ω/z ratios.

A limitation of MALDI for peptide mass mapping is that some peptides do not ionize well and therefore are not detected by the mass spectrometer.[58] A comparison of the relative abundances for the $[M + H]^+$ ions of each peptide obtained at high pressure suggests that discrimination in the ionization process is less for high-pressure MALDI. A high-vacuum MALDI mass spectrum is shown in Figure 4B. Note that formation of angiotensin II ions is suppressed in the presence of other peptides; however, abundant $[M + H]^+$ ions of angiotensin II are detected by high-pressure MALDI. Although we have not exhaustively compared discrimination effects for the two MALDI experiments, we generally observe less discrimination for high-pressure MALDI of protein digest samples.[59]

Figure 5 contains a three-dimensional plot of mass spectra as a function of mobility drift time for a tryptic digest of thermally denatured[54] chicken egg white lysozyme acquired on the IM-oTOF instrument. The 3-D plot was assembled from individual calibrated mass spectra using the multifile program included in Grams/32. The labeled and identified digest fragments are listed in Table 1 along with the average masses and corresponding amino acid sequence. Coverage is indicated by the highlighted amino acids in the listed protein sequence. The mass spectral peaks follow a trend line indicating a near linear dependence of drift time versus m/z for m/z values below ~1500 followed by a nonlinear relationship for higher m/z ratios. Figure 6 shows a high-vacuum mass spectrum of the same tryptic digest obtained by using a high-resolution time-of-flight mass spectrometer in linear mode. The labeled and identified fragments are listed in Table 2 along with the average masses and corresponding amino acid sequence. Coverage is indicated by the highlighted amino acids in the listed protein sequence.

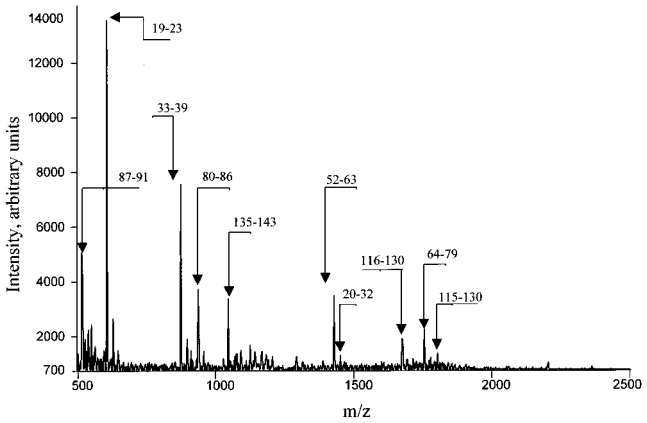

Figure 6. High-vacuum MALDI mass spectrum of a tryptic digest of thermally denatured chicken egg white lysozyme.

A distinct advantage of the IM-oTOF-MS peptide mass mapping is the reduction of chemical noise afforded by the separation process prior to mass analysis. We attribute the increased coverage for the high-pressure experiments (97% amino acid coverage for IM versus 55−60% for high-vacuum MALDI, see Tables 1 and 2) to a reduction in the amount of noise in the mass spectrum. Using the IM-oTOF-MS, we are able to see low-abundance peptide fragments that are buried in the noise of the high-vacuum MALDI experiment.

CONCLUSION

The objective for many IM studies has been to obtain the highest resolution possible in order to separate different conformers of peptides and/or isomeric molecules; however, our approach

(58) Cohen, S. L.; Chait, B. T. *Anal. Chem.* **1996**, *68*, 31−37.
(59) Ruotolo, B.; Gillig, K. J.; Stone, E.; Russell D. H., manuscript in preparation.

has been to combine high-pressure MALDI, which produces simple mass spectra consisting primarily of singly charged protonated molecules, with low-resolution IM, which is adequate for separating digest fragments. Acquiring spectra in the mass mode and scanning through the mobility spectrum introduces a dimensionality that is similar to that of 2D-gel electrophoresis. The IM separation occurs on a time scale that is compatible with the acquisition of mass spectral data. Additionally, MALDI-IM reduces problems associated with contamination and signal suppression from salts and detergents leftover from 2D-PAGE separation and the subsequent process of cleaning up the 2D-gel "spot". In the future, we envision complex mixture analysis while operating the drift cell at higher pressures to simplify the identification of proteins in protein mixtures. For example, by simultaneously obtaining Ω/z and m/z ratios the resulting data can be used for many applications in proteomics.

The IM-o-TOF instrument described herein can be operated as a tandem TOF mass spectrometer. For example, the ion drift time through the mobility cell is proportional to the molecular weight of the analyte; e.g., IM is used as a low-resolution mass spectrometer. Activation and dissociation of the mobility separated ions followed by mass analysis of the corresponding fragment ions is equivalent to MS−MS. Preliminary experiments[60] suggest that surface-induced dissociation (SID)[61] can be used to sequence proteolytic digest fragments, and Clemmer et al. have recently shown that collision-induced dissociation (CID) can also be used for the same purpose.[62]

The spectrum of gramicidin S shown in Figure 2b suggests that the IM-o-TOF has excellent sensitivity (at least 10 fmol in idealized cases) and although adequate for peptide mass mapping we do not feel that the prototype instrument is yet optimized. Improvements to the drift cell and IM-o-TOF interface can certainly increase the sensitivity by 1−2 orders of magnitude. Thus, we anticipate limits of detection (LODs) that range from 0.1 to 1 fmol of peptide. Furthermore, we are confident that the detection limits can be achieved for peptide mixtures, e.g., proteolytic digests.

ACKNOWLEDGMENT

The ion mobility research at TAMU is supported by a grant from the National Science Foundation (CHE-9629966) and the TAMU TOF-MS development research is supported by the U.S. Department of Energy, Division of Chemical Sciences, OBES. The ion mobility/o-TOF MS developed at Ionwerks Inc. was funded by a NIH Phase 1 SBIR grant (1R43 GM057736-01).

Received for review May 16, 2000. Accepted July 12, 2000.

AC0005619

(60) Stone, E.; Gillig, K. J.; Ruotolo, B.; Russell D. H., manuscript in preparation.
(61) Cooks, R. G.; Ast T.; Mabud, A. *Int. J. Mass Spectrom. Ion Processes* **1990**, *100*, 209−265.
(62) Clemmer, D. E.; Hoaglund Hyzer, C. S. Presented at Pittsburgh Conference, New Orleans, LA., March 14, 2000; paper 353.